



# Novel BECCS implementation integrating chemical looping combustion with oxygen uncoupling and a kraft pulp mill cogeneration plant

Jussi Saari<sup>1</sup> · Petteri Peltola<sup>1</sup> · Katja Kuparinen<sup>1</sup> · Juha Kaikko<sup>1</sup> · Ekaterina Sermyagina<sup>1</sup> · Esa Vakkilainen<sup>1</sup>

Received: 3 October 2022 / Accepted: 14 March 2023 / Published online: 29 March 2023  
© The Author(s) 2023

## Abstract

Bioenergy with CO<sub>2</sub> capture and storage (BECCS) is a promising negative emission technology (NET). When using sustainably produced biomass as fuel, BECCS allows the production of power and heat with negative CO<sub>2</sub> emissions. The main technical challenges hindering the deployment of BECCS technologies include energy penalties associated with the capture process. This work evaluates the performance of an advanced CO<sub>2</sub> capture technology, chemical looping with oxygen uncoupling (CLOU), replacing a conventional fluidized bed boiler in the power boiler role in a large, modern integrated pulp and paper mill. Results from a MATLAB/Simulink reactor model were incorporated in a plant and integration model developed in a commercial process simulation software to quantify the performance of the CLOU-integrated cogeneration plant. The results show that in this specific application, the typically already low efficiency penalty of CLOU-based carbon capture and storage (CCS) systems could be eliminated entirely, and actually even a very small efficiency gain could be obtained. The highly efficient operation is possible due to the high moisture and hydrogen contents of the biomass and the separation of combustion products and excess air streams in the CLOU process; this provides an opportunity to recover a significant amount of heat by flue gas condensation at a higher temperature level than what is possible in a conventional boiler. Together with abundant low-temperature heat sinks available at the pulp and paper application allows freeing a considerable amount of low-pressure steam for expansion in the condensing turbine. The resulting increase in gross generator output proved enough to not only match, but very slightly exceed the approximately 18 MW parasitic load introduced by the CLOU system in comparison to the conventional boiler.

**Keywords** Bioenergy with carbon capture and storage (BECCS) · Chemical looping combustion with oxygen uncoupling (CLOU) · Climate change mitigation · Negative CO<sub>2</sub> emission technologies (NETs) · Cogeneration · Pulp and paper industry

---

✉ Jussi Saari  
saari@lut.fi

Extended author information available on the last page of the article

## Nomenclature

$h$	Specific enthalpy (kJ/kg)
$\Delta H$	Reaction enthalpy (kJ/mol)
$k_1$	Pre-exponential factor (1/(atm s))
$k_2$	Activation energy (J/mol)
$LHV$	Lower heating value (MJ/kg)
$\dot{m}$	Mass flow rate (kg/s)
$p$	Pressure (Pa, bar, atm)
$P_{el}$	Electric power (MW)
$r$	Reaction rate (1/s)
$R_u$	Universal gas constant, 8.3145 kJ/kmolK
$SE_{CO_2}$	Specific CO <sub>2</sub> emission (kg/MWh <sub>el</sub> )
$T$	Temperature (°C, K)
$\dot{V}$	Volumetric flow rate (m <sup>3</sup> /s)
$X_{OC}$	Oxygen carrier conversion degree (-)

## Greek symbols

$\beta$	Reaction order (-)
$\phi_{fg}$	Flue gas recirculation ratio (-)
$\Phi$	Heat rate; thermal power (W)
$\eta_c$	Compression efficiency (-)
$\eta_{el}$	Electric efficiency (-)
$\eta_{em}$	Electric motor efficiency (-)
$\lambda$	Excess air ratio (-)

## Acronyms

ADt	Air dried tonne
AR	Air reactor
BECCS	Bioenergy carbon capture and storage
CCS	Carbon capture and storage
CCU	Carbon capture and utilization
CDR	Carbon dioxide removal
CFB	Circulating fluidized bed
CHP	Combined heat and power
CLC	Chemical looping combustion
CLOU	Chemical looping combustion with oxygen uncoupling
COP	Coefficient of power
CPU	Compression and purification unit
DA	Deaerator
daf	Dry ash-free
ETS	Emission trading system
FG	Flue gas
FDF	Forced draft fan
FGC	Flue gas condenser
FR	Fuel reactor
FW	Feedwater
GHG	Greenhouse gas
GS	Governing stage

HP	High pressure
HPFH	High-pressure feed heater
HPT	High-pressure turbine
IDF	Induced draft fan
IEA	International energy agency
IGCC	Integrated gasification combined cycle
IPCC	International panel on climate change
KRB	Kraft recovery boiler
LHV	Lower heating value
LP	Low pressure
LPT	Low-pressure turbine
MC	Moisture content
MDK	Model Development Kit
MEA	Monoethanolamine
MP	Medium pressure
NET	Negative emission technology
PCC	Precipitated calcium carbonate
PPI	Pulp and paper industry
SCAH	Steam coil air heater
SG	Steam generator
SH	Superheater
TG	Turbogenerator
TRL	Technical readiness level
wb	Wet basis

### Subscripts

aux	Auxiliary
c	Compression
el	Electric
em	Electric motor
f	Fuel
FW	Feedwater
HP	Heat pump
m	Mechanical
TG1	Turbogenerator 1
TG2	Turbogenerator 2
tot	Total

## 1 Introduction

The goal of limiting global warming below 2 °C defines a strictly limited carbon budget, which appears very likely to be overshoot given the still increasing rate of CO<sub>2</sub> emissions and the clear difficulty of agreeing to the rapid reductions that would be required to stay within the carbon budget by emission reductions alone. To stay within a carbon budget to meet the below 2 °C goal, and particularly the stricter goal of below 1.5 °C warming, carbon dioxide removal (CDR) from atmosphere is thus clearly required (de Coninck et al. 2018). Several negative emission technologies (NETs) have been proposed, of which

bioenergy with carbon capture and storage (BECCS) is beginning to emerge as one of the most promising in terms of both cost-effectiveness and carbon removal potential (Fajardy et al. 2021).

Within the broad category of BECCS, several potential technologies exist; the most studied technology is currently the monoethanolamine (MEA) scrubbing post-combustion process (Karjunen et al. 2017). MEA scrubbing is a commercially available post-combustion technology but suffers from the disadvantage of considerable efficiency penalty due to the steam and power consumptions of the scrubbing system. Retrofitting existing power plants with MEA scrubbing is considered relatively simple because the capture unit can be added downstream of the boiler with minimal modifications to the original plant. Other post-combustion methods promising reduced parasitic loads in comparison to MEA scrubbing are being developed, e.g. calcium looping (CaL), membrane separation and cryogenic separation, but the relatively low CO<sub>2</sub> concentration of only 10...15 vol% in the wet flue gases from solid-fuel boilers inevitably increases the energy demand of post-combustion CCS processes over what would be possible with more concentrated streams (Bandilla 2020).

Processes that yield more concentrated CO<sub>2</sub> streams than conventional combustion would result in reduced efficiency penalties. Such examples include pre-combustion separation in an integrated gasification combined cycle (IGCC), oxy-combustion and chemical looping combustion (CLC), but the cryogenic air separation units for producing the oxygen needed by both oxy-combustion and oxygen gasification step of the IGCC-based pre-combustion separation still represent a significant parasitic load leading to considerable efficiency penalties with these technologies as well. Oxy-combustion can be applied to industry-standard pulverized coal combustion plants with moderate changes to the original plant, while a complete change in base plant technology is required for pre-combustion capture in IGCC plants (Toftegaard et al. 2010).

CLC is a promising technology that allows separating the CO<sub>2</sub> from the combustion process at a comparatively low cost and efficiency penalty (Adánez et al. 2018). Typically, this would be implemented by two interconnected fluidized bed reactors, the air reactor (AR) and the fuel reactor (FR), with a solid metallic oxide oxygen carrier circulating between them. The oxygen carrier is oxidized in the AR and transported to the FR, where it reacts with the fuel. The hydrocarbon fuel is oxidized to water and carbon dioxide while releasing heat; the hot flue gas is removed through a cyclone to heat recovery, while the solid oxygen carrier is returned to the AR to be fully oxidized again. Gas flow from the AR is mainly nitrogen and excess oxygen with trace amounts of impurities from combustion, while the FR gas stream consists mainly of the combustion products, water vapour and carbon dioxide. Finally, a sequestration-ready CO<sub>2</sub> stream is obtained after the removal of water by condensation. As the CO<sub>2</sub> is inherently separated from the other flue gas components, the entropy-related gas separation work requirement common to most other CO<sub>2</sub> capture approaches is avoided, yielding no efficiency penalty more than that required for compression of the product.

Chemical looping with oxygen uncoupling (CLOU) is one variant of CLC better suited for use with solid fuels. A CLOU process uses an oxygen carrier that spontaneously releases gas-phase oxygen in atmospheric pressures at temperature ranges relevant for combustion (Mattisson et al. 2009). Earlier studies have indicated that in a conventional fossil coal-fired condensing power plant application, CLOU system would have significant performance advantages over oxy-combustion or MEA absorption, with much lower efficiency penalties (Spinelli et al. 2016). In the context of BECCS and particularly a cogeneration application thereof, with significant low-temperature heat sinks

and a fuel characterized by higher moisture and hydrogen contents than what is typical for fossil fuels, the CLOU appears particularly advantageous, as the separation of not only CO<sub>2</sub> but also H<sub>2</sub>O in their separate, undiluted stream, allows also much more efficient condensing flue gas heat recovery than what is possible in a conventional boiler (Peltola et al. 2020). An earlier study investigating a district heat back pressure implementation with a two-stage heat recovery scheme reported an efficiency penalty of as little as 0.7% (Saari et al. 2020).

The technical readiness level (TRL) of CLC technology in solid-fuel combustion is currently at or approaching 6 (Peltola et al. 2022). The largest solid-fuel experimental units the authors are aware of are a 3 MW<sub>th</sub> unit in the USA (Abdulally et al. 2014) and a 1 MW<sub>th</sub> unit in Darmstadt, Germany (Ströhle et al. 2014). CLOU combustion of solid biomass with the cuprous/cupric oxide oxygen carrier considered in this work has been demonstrated in 1.5 kW<sub>th</sub> unit (Adáñez-Rubio et al. 2014).

In this study, a novel coupling of CLOU process and the cogeneration steam cycle of a modern integrated pulp and paper mill is presented. The pulp and paper sector is the largest industrial bioenergy user (IEA 2022) and a notable producer of energy, especially bioenergy. Most of the produced pulp is chemical (kraft) pulp. In the kraft pulp production process, about half of the wood raw material ends up in the product, while the other half is used for bioenergy. The magnitude of the pulping sector is not always fully understood: the recovery boilers, apart from being a part of the kraft pulp production process, are also one of the largest boiler types converting biomass to energy (Vakkilainen et al. 2013). In addition to the recovery boiler, a kraft pulp mill has other CO<sub>2</sub> point sources, of which the largest ones, after the recovery boiler, are the lime kiln and, in most mills, the power boiler producing additional energy by combusting residual biomass. In modern mills, the lime kiln is often the only source of fossil CO<sub>2</sub> (Vakkilainen and Kivistö 2014), although substituting fossil fuels with renewables also in lime kilns has been a recent trend in many mills (Lipiäinen et al. 2022). The large pulp and paper units with their already existing biogenic CO<sub>2</sub> point sources offer the attractive possibility to apply BECCS without additional biomass harvesting, which tackles the common concern over large-scale implementation of BECCS resulting in land-use increase.

The technical potential to capture CO<sub>2</sub> from pulp mills is substantial: approximately 137 MtCO<sub>2</sub>/a could be removed from the atmosphere by applying carbon capture in the existing pulp mills (Kuparinen et al. 2019). The large unit size of the pulp and paper processes offers an additional advantage, as economies of scale are one of the main factors affecting the costs of carbon capture (Kearns et al. 2021). Previous studies on capturing biobased CO<sub>2</sub> from the outgoing flows of pulp and paper mills have mainly focused on technical feasibility of MEA absorption (Onarheim et al. 2017a; Kuparinen et al. 2019); estimation on costs (Onarheim et al. 2017b; Karjunen et al. 2017); or the possible scale or emission reduction potential (Leeson et al. 2017; Kuparinen et al. 2019; IEA 2020).

The pulp and paper mill was considered a particularly promising application for the suggested CLOU system, as industrial cogeneration load profiles are relatively constant and stable, and the pulp mill hot water users provide a suitable heat sink for the heat recovered hot water from the FR gas stream. As the pulp and paper industry (PPI) is looking for additional revenue streams (Hamaguchi et al. 2013), and several potential on-site uses for the captured CO<sub>2</sub> have been identified (Kuparinen et al. 2019; 2021), the pulp and paper mill has advantages from the perspective of carbon capture and use (CCU) as well. The configuration considered in this study is based on a reference case where the bark residues of the mill are combusted in a 280 MW<sub>LHV</sub> circulating fluidized bed (CFB) boiler. The performance of the BECCS implementation is compared to this reference case.

The CLOU reactor performance is modelled using a MATLAB/Simulink model developed earlier for fluidized bed boiler and reactor modelling (Peltola et al. 2013a), while the steam cycle and heat recovery systems are modelled with IPSEpro process modelling software using component models described in Saari et al. (2018).

Only direct CO<sub>2</sub> emissions are considered here. For multiple reasons, indirect and non-CO<sub>2</sub> greenhouse gas (GHG) emissions are ruled beyond the scope of the study: firstly, the emissions of biogenic CO<sub>2</sub> from chemical pulping, where electricity purchase is not needed, exceed the indirect emissions by an order of magnitude (Ericsson & Nilsson 2018); secondly, the GHG emissions of non-CO<sub>2</sub> gases from kraft mills are typically of even lower in magnitude (EPA 2009); and finally, the non-CO<sub>2</sub> GHG emissions both originate mostly from sources unrelated to the power boiler (EPA 2009), thus being unaffected by the investigated replacement of a power boiler with a CLOU reactor system.

## 2 Methods

The study was conducted by considering the case of a modern Nordic integrated pulp and paper mill with a 280 MW<sub>LHV</sub> CFB power boiler for the combustion of bark and other solid residues from the wood handling and other mill processes. The mill is approximately based on the Mill A described by Kuparinen et al. (2019), with similar live steam values in both boilers and identical power boiler fuel composition and heating value. The main difference is that whereas the Mill A of Kuparinen et al. (2019) produces 1.4 million ADt of pulp annually, with an additional import of 0.1 million ADt for the paper mill to produce 4224 t/d of paper, the mill considered here produces 1.6 million ADt of pulp for 3750 t/d paper production and 0.3 million ADt/a pulp export. The specific power and steam consumptions of both mills are similar, with the slightly different capacities of the pulp and paper mills resulting in slightly different breakdown between the two, but near-identical total sum of power consumption between this work and that by Kuparinen et al. (2019). In terms of the power boiler and the steam cycle, the main difference is that whereas the Mill A (Kuparinen et al. 2019) lacks high-pressure feed heaters, resulting in feedwater temperature of 120 °C, in this study, a single high-pressure closed feed heater is assumed, for a 186 °C feedwater temperature.

The steam cycle of the mill was modelled using IPSEpro simulation software, both using the original configuration with the conventional CFB boiler, and with a CLOU reactor pair replacing the conventional boiler in order to evaluate the technical performance achievable in such configuration. The following chapters describe the modelling methodology used.

### 2.1 Modelling software

The boiler, steam cycle and heat recovery equipment are modelled using IPSEpro, a steady-state, equation-oriented commercial process simulation software for simulation and design of power plants (Dargam and Perz 1998) by SimTech GmbH, Graz, Austria. In the IPSEpro environment, the overall plant flowsheet models are constructed using discrete modules representing individual power plant and boiler components, which are connected by streams. Each component model consists of a set of equations describing the behaviour of the component. These equations, together with any additional free equations the user may define, form the system of nonlinear equations that is the plant model. This is solved in IPSEpro by first dividing the equations into groups and then solving the groups consecutively with a Newton–Raphson-based solver (Häggeståhl and Dahlquist 2003).

The IPSEpro software includes a Model Development Kit (MDK), which allows modifying the existing standard library components, or creating new component modules not included in the standard power plant component library. The MDK was used to create the recovery boiler furnace module and the spray tower and humidifier modules used in this study.

To increase the reliability of the plant model results, the behaviour of the considered dual-CFB CLOU system was first evaluated using a 1.5D core-annulus-type model frame applicable to chemical looping processes. The outputs from this—the reactor cooling rates and outlet gas mass flow rates, temperatures and compositions—are employed as inputs to the plant model implemented in IPSEpro. The reactor model is implemented in a MATLAB/Simulink environment, where different components of the reactor system are linked to form a flowchart for the overall process. The reactor models are based on mass and energy balances, as well as semi-empirical correlations for the calculation of gas–solid hydrodynamics, chemical reactions and heat transfer. A core-annulus-type approach has been applied to describe the flow of solids in the reactors, hence the notation 1.5D. Steady-state operating conditions are obtained by solving a set of time-dependent equations with Simulink's ordinary differential equation solver. The model allows simulating both the air and fuel reactors in the CLOU loop. A more detailed description of the 1.5D model is provided in references (Peltola et al. 2015; 2013a). The model can be utilized as a tool for preliminary reactor design (Peltola et al. 2015) as well as for predicting the performance of large-scale systems (Spinelli et al. 2016; Peltola et al. 2013b).

## 2.2 Considered mill and the steam cycle

The integrated pulp and paper mill, described by Kuparinen et al. (2019), represents a large, modern mill producing 1.6 million ADt/a of bleached pulp from softwood. Steam is used firstly in the mill processes and for electricity generation. The mill is self-sufficient in energy and able to sell excess electricity. The pulping process, recovery boiler and related steam and power production are similar to those of the pure pulp mill considered in Saari et al. (2021). The case considered here differs from that of Saari et al. (2021) in having an integrated paper mill producing coated and uncoated paper. The paper mill is a notable additional consumer of both power and heat (steam), and to supply these, there is an additional separate biomass boiler.

Residues from the wood handling process, 88.2% softwood bark and 11.8% fine wood residues by mass, are combusted in the biomass boiler. To permit higher steam values for the biomass boiler, both boilers have their own separate turbogenerators, but partially share the condensate system in having common production of demineralized makeup water and a common deaerator and feedwater tank. Flowsheet model of the CHP plant of the integrated pulp and paper mill was implemented in IPSEpro. Table 1 shows the main parameters; power boiler fuel composition is listed in Table 2.

### 2.2.1 Boiler, steam cycle and heat recovery models

The flowsheet of the boiler and steam cycle models can be seen in Fig. 1. Both turbines have partial-admission governing stages with design-point isentropic expansion efficiencies  $\eta_s$  of 0.70 and pressure ratios of 0.6 with valves wide open. This is followed by a HP back pressure turbine,  $\eta_s=0.909$  and a back pressure of 5 bar(a), corresponding to the pressure level of the LP steam for the pulp and paper mills. Both turbines have HP,

**Table 1** Integrated pulp and paper mill main parameters. KRB refers to the kraft recovery boiler and CFB to the circulating fluidized bed power boiler whose replacement by a CLOU system is studied

Category	Parameter	Value	
Production	Operating hours (h/a)	8400	
	Pulp production ( $t_{AD}/a$ )	1.6·10 <sup>6</sup>	
	Paper production (t/d)	3750	
Energy	Steam use, pulp mill (t/h)	775	
	Steam use, paper mill (t/h)	355	
	Power generation ( $MW_{el, gross}$ )	258	
	Power use, pulp mill ( $kWh/t_{AD}$ )	552	
	Power use, paper mill ( $kWh/t$ )	681	
Boiler	Boiler	KRB	CFB
	Dry solids to boiler ( $t_{ds}/d$ )	7997	1475
	Dry solids $x_{ds}$ , firing liquor (-)	0.82	n/a
	Main steam production (t/h)	1050	309
Turbogenerator	Turbogenerator	TG1	TG2
	Turbine inlet temperature (°C)	500	550
	Turbine inlet pressure (bar)	100	117
	Condensing tail	No	Yes

**Table 2** Boiler fuel properties

Proximate analysis ( $m_d\%$ )		Ultimate analysis ( $m_{daf}\%$ )	
Volatile	74.2	C	53.11
Fixed Carbon	24.3	H	5.82
Ash	1.5	O	40.67
Heating value (MJ/kg)		N	0.37
HHV <sub>daf</sub>	20.151	S	0.03
LHV <sub>af</sub>	8.079	Σ	100.00

MP2 and MP1 extractions, at pressure levels of 27, 18 and 12 bar(a), respectively. The TG1 of the recovery boiler has a pure back pressure turbine, while the TG2 of the CFB boiler includes a condensing tail with 30 kg/s swallowing capacity; at design point, it operates with 25.4 kg/s steam flow and 4.5 bar(a) inlet pressure and 25 mbar pressure at the vacuum condenser.

Determining the variation of turbine pressure levels and as a function of varying flows is based on the ellipse law by Traupel (1966). The expansion efficiency variation is based on the correlation presented by Jüdes et al. (2009) with a correction for possible moisture in the wet steam region according to Sanders (2004). The methodology of calculation is described in more detail in Saari et al. (2018).

The reference plant CFB boiler is modelled with four main types of modules: the CFB furnace, superheater (labelled “SH” in Fig. 1), economizer (“Eco”) and air pre-heater (“Luvo”). The furnace module contains a simple steam generator heat transfer model based on an average furnace temperature and heat transfer coefficient, according to Basu (2006), as well as a small additional superheater surface, a so-called INTREX superheater in the bottom of the return leg, used to obtain an increased final superheated steam temperature in some biomass-fired steam boilers. All boiler losses except for the



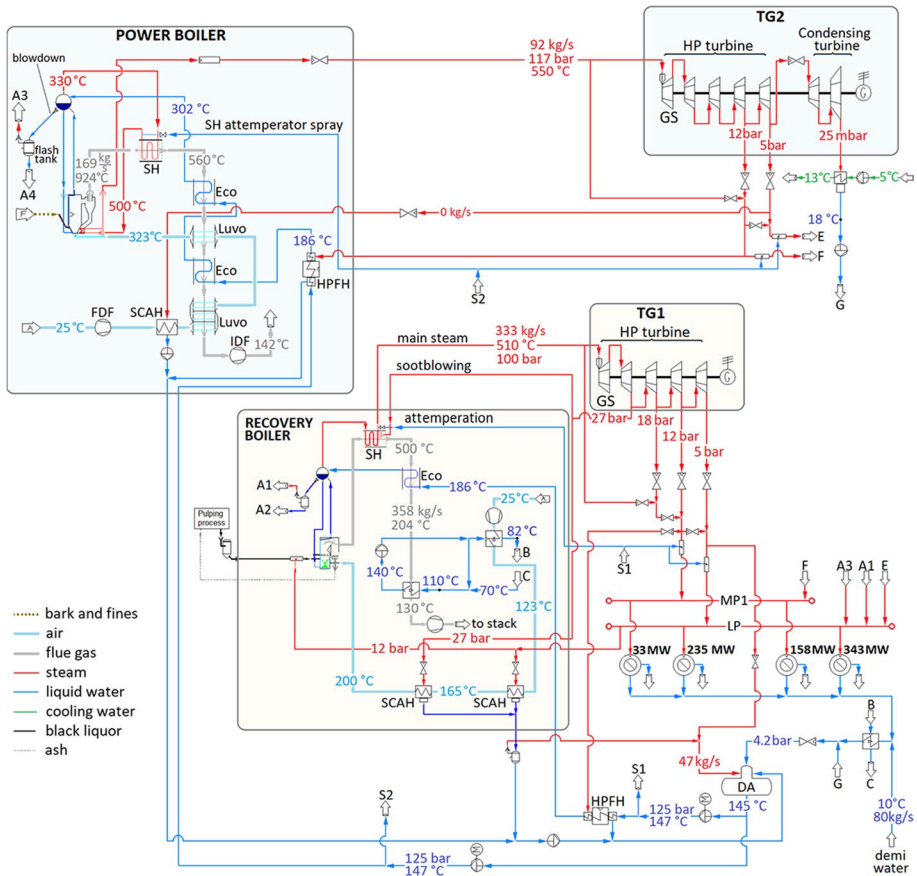


**Fig. 1** Flowsheet model of the pulp and paper mill CHP plant

stack loss are also determined in the furnace module. The superheater, economizer and air preheater are each represented by a single heat exchanger component. A steam coil air heater (SCAH) is present so that a stack temperature sufficient to prevent acid condensation can always be maintained. One percent of the feedwater flow rate is removed as blowdown from the drum. The blowdown is depressurized to 5 bar(a), and the flash steam is used to augment the LP steam supply. The recovery boiler calculation is based on Vakkilainen (2005) and described by Saari et al. (2021) and Vakkilainen (2005); black liquor composition from the pulping process is identical to that of Saari (2021).

In the IPSEpro CLOU plant model, the CFB furnace module is replaced with a CLOU reactor module, which takes the results of the separate CLOU reactor simulation as manual input, and gives out the gas streams of specified composition, state and flow rate. The steam generator and superheater surfaces located in the air and fuel reactors are considered by specifying the cooling rates, obtained as output of the reactor model, into the IPSEpro plant model’s reactor module.

The flue gas condenser (FGC) for removing excess water from the fuel reactor gas stream and heat recover is modelled as a three-stage spray tower design similar to that

described in Saari et al. (2020) and Saari et al. (2021), shown in Fig. 2. The first stage is a venturi scrubber, which serves the dual purposes of both cleaning the gas and cooling it down considerably so as to permit smaller size and lower-cost materials to be used in the packed bed heat recovery scrubbers. NaOH injection to spray water can be used for pH control. Evaporation rather than condensation takes place in the first stage, which together with cooling leads to little net energy transfer to the gas stream. The condensation and heat recovery then take place in a two-stage packed bed scrubber system. Each of the three scrubber stages is modelled as separate unit in the flowsheet model.

### 2.3 CLOU reactor model

There is a limited set of metal oxides having suitable equilibrium partial pressures of oxygen at temperatures relevant for combustion to facilitate oxygen release in the fuel reactor. In this study, copper oxide,  $\text{CuO}/\text{Cu}_2\text{O}$ , was considered the oxygen carrier. The advantages of  $\text{CuO}/\text{Cu}_2\text{O}$  include high reactivity, high oxygen transport capacity and lack of thermodynamic limitations for the complete hydrocarbon combustion (Mattisson 2013). The oxygen carrier was used as a 50:50 mixture of active  $\text{CuO}/\text{Cu}_2\text{O}$  and supporting  $\text{TiO}_2$ , with physical properties representing Geldart B particles (100- $\mu\text{m}$  average particle size, 4650  $\text{kg}/\text{m}^3$  apparent density). In the CLOU regime, copper cycles between the cupric  $\text{CuO}$  and cuprous  $\text{Cu}_2\text{O}$  state,

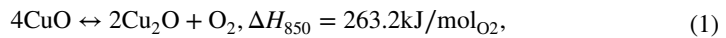
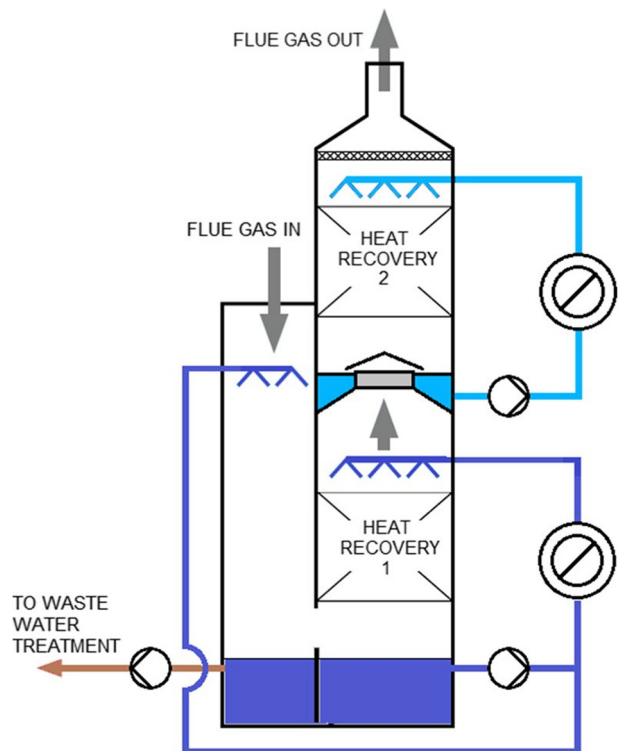


Fig. 2 Flue gas condenser



where  $\Delta H_{850}$  is the reaction enthalpy at 850 °C temperature.

In the FR, the CuO undergoes an endothermic reduction reaction to release oxygen, while the biomass particles undergo devolatilization, and combustion takes place with the gaseous oxygen. The net reaction is exothermic. The oxygen carrier is then transferred in its reduced form  $\text{Cu}_2\text{O}$  to the AR, where it is re-oxidized back to CuO in an exothermic reaction.

The oxidation and decomposition of the oxygen carrier are both affected by a thermodynamic driving force, which is governed by the difference between the partial pressure of oxygen in a reactor,  $p_{\text{O}_2}$ , and the equilibrium  $p_{\text{O}_2}$ . The equilibrium curve for a CuO/ $\text{Cu}_2\text{O}$  system is shown in Fig. 3. A detailed description of the oxygen carrier redox model used in this work is found in Spinelli et al. (2016). For both CuO reduction and  $\text{Cu}_2\text{O}$  oxidation, a conversion rate equation can be formulated as

$$r = f(T)f(X)f(p_{\text{O}_2}, p_{\text{O}_2,\text{eq}}), \quad (2)$$

where  $f(p_{\text{O}_2}, p_{\text{O}_2,\text{eq}})$  represents the role of the thermodynamic driving force,  $f(X)$  accounts for the reaction mechanism and  $f(T)$  expresses an Arrhenius-type dependency on temperature. The OC oxidation and reduction kinetics as applied in the air and fuel reactors are shown in Table 3, and the model for solid-fuel combustion is described in Peltola et al. (2015). The rate expression and kinetic parameters for biochar oxidation were obtained from Champion et al. (2014).

Reactor performance has a significant impact on plant performance: a fuel conversion reduction of 2 percentage points typically reduces the  $\eta_{\text{net}}$  of the plant by 1 percentage point (Peltola et al. 2013b). The procedure to determine the reactor characteristics and operating conditions in this study is mostly similar to that presented in Spinelli et al. (2016).

The CLOU reactor system employed in this work is shown in Fig. 4. Both the AR and FR are designed as atmospheric-pressure CFBs and operated in the high-velocity regime, enabling gas–solid contact throughout the reactor height for maximum fuel conversion. Compared to other reactor configurations, this design has many advantages (Peltola et al. 2013b). The AR is fluidized with preheated air, and the FR with partially recirculated flue gas. The FR gas wet basis recirculation ratio is defined as

**Fig. 3** Equilibrium partial pressure of oxygen over the CuO/ $\text{Cu}_2\text{O}$  system

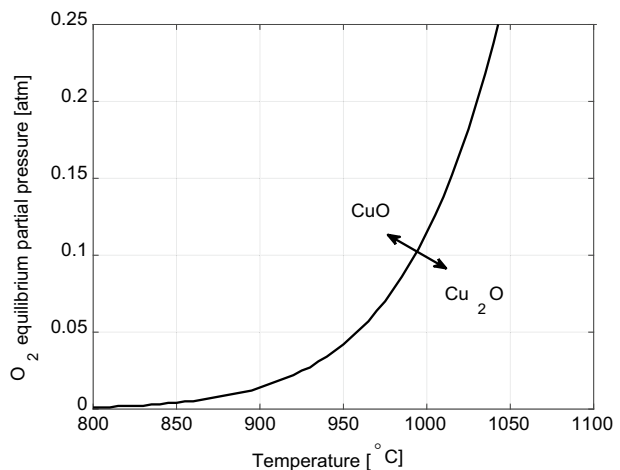


**Table 3** Functions and constant parameters of oxygen carrier oxidation and reduction kinetics

Item	Oxidation: air reactor (Clayton et al. 2014)	Reduction: fuel reactor (Clayton and Whitty 2014)
$f(X)$ (-)	$1 - X_{OC}$	$X_{OC}$
$f(p_{O_2}, p_{O_2,eq.})$ ( $\text{atm}^\beta$ )	$(p_{O_2}^\beta - p_{O_2,eq.}^\beta)$	$(p_{O_2,eq.}^\beta - p_{O_2}^\beta)$
$f(T)$ ( $1/(\text{atm}^\beta \text{ s})$ )	$k_1 e^{\frac{-k_2}{R_u T^a}}$	$k_1 e^{\frac{-k_2}{R_u T^a}}$
$p_{O_2,eq.}$ (atm)	$6.057 \cdot 10^{-11} e^{0.02146 T^b}$	$6.057 \cdot 10^{-11} e^{0.02146 T^b}$
$k_1$ ( $1/(\text{atm}^\beta \text{ s})$ )	$5.60 \cdot 10^4$	$4.15 \cdot 10^4$
$k_2$ (J/mol)	$6.8 \cdot 10^4$	$6.7 \cdot 10^4$
$\beta$ (-)	1.3	1.3

<sup>a</sup>(T) = K

<sup>b</sup>(T) = °C

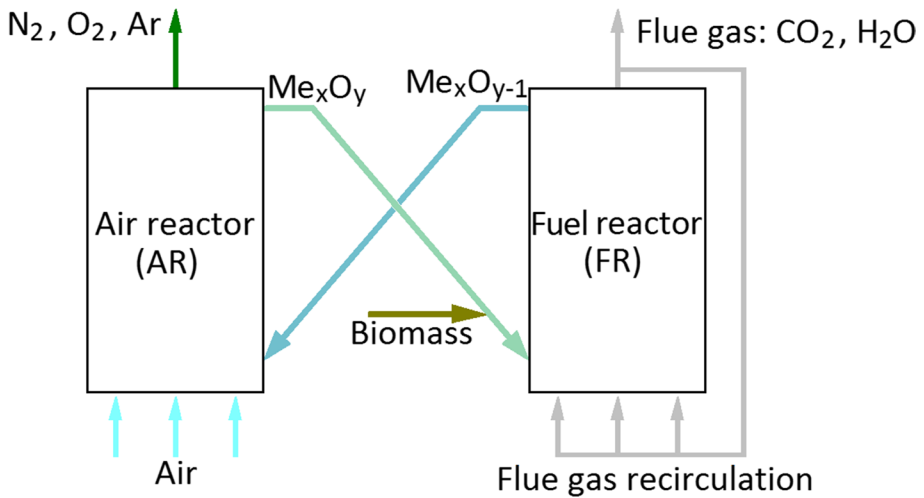


**Fig. 4** Schematic drawing of the CLOU reactor system

$$\phi_{fg} = \frac{\dot{m}_{recirc}}{\dot{m}_{FR,out}}, \tag{3}$$

where  $\dot{m}_{recirc}$  is the recirculation mass flow rate and  $\dot{m}_{FR,out}$  is the total flow exiting the FR. When determining the recirculation ratio, the formation of combustion gases along the reactor height must be considered. Recirculation gas is cooled to below 450 °C before returning to the FR. The cross-sectional areas of the reactors were sized to obtain the desired gas velocities.

The reaction kinetics and the equilibrium  $p_{O_2}$  depend heavily on temperature; the operating temperatures of the reactors are thus important. Temperatures of 900–950 °C have

been identified as suitable for CuO-based oxygen carriers (Abad et al. 2012). At typical CLC/CLOU operating conditions, approximately 50% of the heat input has to be extracted from the reactor system (Abad et al. 2012). The height of the reactors is determined by the heat transfer area required for cooling, as well as ensuring that there is space on the side wall for the particle separator and return systems.

The amount of bed material in each reactor should be minimized to reduce fan power consumption and the size and investment cost of the reactors. The oxygen carrier loading that is required in the system for effective combustion depends on the CuO reduction, Cu<sub>2</sub>O oxidation and fuel combustion kinetics. In the current case, a total solid loading of 534 kg/MW<sub>th</sub> was considered sufficient for >95% fuel conversion (Peltola et al. 2015; Spinelli et al. 2016). A carbon stripper to remove unreacted char from the solid stream from FR to AR was considered unnecessary: the reactivity of biomass char particles allows CO<sub>2</sub> capture efficiencies of over 95% (Peltola et al. 2013a).

The ash generated in the combustion must be periodically purged to avoid accumulation in the reactor system, although this will lead to some loss of the oxygen carrier. An excessive accumulation of the ash in circulating oxygen carrier can be prevented by a proper cyclone design and by employing other particle separation techniques (Whitty 2012). In the current layout, 50% of the ash that accumulates in the solids stream is removed after the air reactor, assuming that the purge stream consists of 99% of ash and 1% of oxygen carrier. With this high selectivity toward ash, the oxygen carrier and ash purge/makeup flows have a negligible effect on the total material and energy balances, as shown by Spinelli et al. (2016). At this point, the assumptions regarding the disposal of ash and separation of oxygen carrier particles from the ash are tentative. This issue involves critical component design aspects, representing an important future research need for CLC/CLOU systems.

## 2.4 Performance metrics

Performance of the investigated BECCS implementation is evaluated in terms of power generation penalty due to the CCS equipment, and CO<sub>2</sub> capture and negative emissions achieved.

The electric efficiency  $\eta_{el,TG2}$  is defined in terms of fuel LHV input,  $\dot{m}_f LHV_f$ , as

$$\eta_{el,TG2} = \frac{P_{el,net,TG2} - P_{aux,TG2}}{\dot{m}_f LHV_f} = \frac{P_{gen,TG2} - P_{aux,TG2}}{\dot{m}_f LHV_f}, \quad (4)$$

where the auxiliary power consumption  $P_{aux,TG2}$  includes the equipment for operating the boiler or CLOU reactors and steam cycle, but not the pulp and paper mill consumptions. The IPSEpro model is used to obtain the power consumptions of boiler or CLOU reactor fans, including feedwater, condensate and condenser cooling water pumps; forced and induced draft fans; fuel reactor flue gas recirculation fan of the CLOU system; and fuel reactor flue gas condensation system pumps and heat pump. The power consumption  $P_{el}$  (kW) of each pump, fan and blower is obtained from

$$P_{el} = \frac{\dot{V} \Delta p}{\eta_c \eta_m \eta_{em}}, \quad (5)$$

where  $\dot{V}$  is the volumetric flow rate (m<sup>3</sup>/s) at the suction side;  $\Delta p$  the pressure increase (kPa); and the  $\eta_c$ ,  $\eta_m$  and  $\eta_{em}$  the compression efficiency, mechanical efficiency and electric motor efficiency, respectively. All pumps, fans and blowers are assumed to be powered

by electric motors, with  $\eta_{em} = 98\%$  and a  $\eta_m = 99\%$ . The compression efficiencies were assumed at 83% for the feedwater pumps, 82% for the induced and forced draft fans and blowers and 81% for the smaller pumps in the systems.

The CLOU system auxiliary power consumption also includes the consumptions of the CO<sub>2</sub> compression and purification unit (CPU) and a heat pump used to upgrade the heat recovered in the FGC system. The CPU power consumption is estimated at 110 kWh/t<sub>CO<sub>2</sub></sub> (Aspelund and Kristin 2007) or 12 MW in this case. The heat pump is assumed to be a compression heat pump using R717 (ammonia, NH<sub>3</sub>). With a temperature lift of less than 20 °C, the coefficient of power (COP) is estimated at 9 based on data by Schlosser et al. (2020). The power consumption  $P_{HP}$  obtained from

$$P_{HP} = \frac{\Phi_{cold}}{COP - 1}, \quad (6)$$

where  $\Phi_{cold}$  is the heat transferred from the heat source (scrubbing water).

Finally, both the reference CFB boiler and the CLOU system are estimated on the basis of Ikonen (2013) to need an additional 1.9 MW to operate various systems not modelled in the IPSEpro flowsheet model, e.g. fuel and ash handling systems, a variety of minor cooling water systems, and the many other minor auxiliary systems of a power plant.

The carbon capture performance is evaluated through specific direct CO<sub>2</sub> emission  $SE_{CO_2}$ ,

$$SE_{CO_2} = \frac{\dot{m}_{CO_2,emitted}}{P_{el,net,TG2}}, \quad (7)$$

## 3 Results

### 3.1 Reactor design

Reactor dimensions and design-point operating conditions in Table 4, obtained as in Spinelli et al. (2016), were used as inputs for 1.5D reactor simulations. The main reactor simulation results are reported in Table 5.

Figure 5 depicts the CLOU reactor system, which replaces the conventional CFB power boiler in the reference case (“power boiler” box in Fig. 1). The back pass heat transfer surfaces are designed so as to obtain the same live steam parameters as in the reference case power boiler. The FR requires some flue gas to be recirculated. To permit affordable materials in the recirculation fan, the recirculation temperature is set at 450 °C. Satisfying these requirements required a somewhat more complex interconnected configuration of heat transfer surfaces than in the basic CFB boiler, as seen in Fig. 5.

Having two separate gas streams, of which one is almost completely devoid of chlorine and water, while the other one must have the water vapour mostly condensed for CO<sub>2</sub> purification purposes, yields opportunities for improved heat recovery and thus efficiency. With the air temperature after the forced draft blower already well above the air reactor gas dew point, it was assumed that the stack temperature would be unlimited by corrosion risk while still using inexpensive materials. In the flue gas stream from the fuel reactor, the exit temperature from the last conventional heat transfer surface, the last air preheater stage, was increased to approximately 200 °C compared to the 142 °C stack temperature of the baseline CHP plant.

**Table 4** Main design and operational parameters of the CLOU system

Parameter	Air reactor	Fuel reactor
Height (m)	28	28
Freeboard cross-section (m <sup>2</sup> )	59.3	50.4
Target gas velocity (m/s)	5–6.5	5–6.5
Air-to-fuel ratio (-)	1.16	n/a
Airflow in (kg/s)	122	n/a
Air temperature (°C)	250	n/a
Specific solids inventory (kg/MW <sub>th</sub> )	267	267
Fuel input (kg/s)	n/a	34.12
Recycle gas ratio (-)	n/a	0.29
Recycle gas input (kg/s)	n/a	24

**Table 5** Main results from CLOU reactor simulation

Parameter	Air reactor	Fuel reactor
Char conversion (-)	0.998	0.961
Solids flux (kg/m <sup>2</sup> /s)	11.5	14.2
OC oxidation degree at outlet (-)	0.941	0.443
Cooling duty (MW)	61.3	41.3
Total pressure drop (kPa)	15.6	18.2
Exhaust gas temperature (°C)	916	935
Exhaust gas mass flow (kg/s)	97.2	58.6*
O <sub>2</sub> (vol%)	2.13	2.85
N <sub>2</sub> (vol%)	95.31	0.06
CO <sub>2</sub> (vol%)	0.60	31.15
H <sub>2</sub> O (vol%)	1.95	65.58
CO, CH <sub>4</sub> , H <sub>2</sub> , SO <sub>2</sub> (vol%)	-	Traces

\*Flue gas fraction that is not recirculated back to the fuel reactor

Figure 6 shows the temperature diagrams of both the FR (Fig. 6a) and AR (Fig. 6b), including the backpass heat exchangers, with that of the original CFB power boiler (Fig. 6c) for comparison. In contrast to the benign AR gas with negligible amounts of combustion products, the FR gas stream has elevated concentrations of chlorine and alkali metals, exacerbating high-temperature corrosion in the superheaters as well as increasing acid dew point at the air preheaters. Consequently, the majority of the superheater and air preheater surfaces were placed at the AR backpass, and most of the economizer surface, having the least risk of corrosion with inexpensive materials, was placed on the FR backpass. Initial preheating of air takes place in the AR surfaces; the 122 °C air entering the last FR air heater is hot enough to prevent condensation even at the inlet, an advantage achieved at the cost of clearly increased FR gas outlet temperature. In the flue gas condenser, sodium hydroxide injection will almost certainly be needed for pH control in order to prevent corrosion problems.

In order to reduce the temperatures at the superheater surfaces, a steam generator bank precedes the first FR superheater, placed in a parallel-flow configuration to further reduce the surface temperatures. The sums of the conductances of the heat transfer surfaces are listed in Table 6; the closer temperature approaches of particularly the AR air preheaters result in greater total conductances than those of the equivalent CFB boiler surfaces.

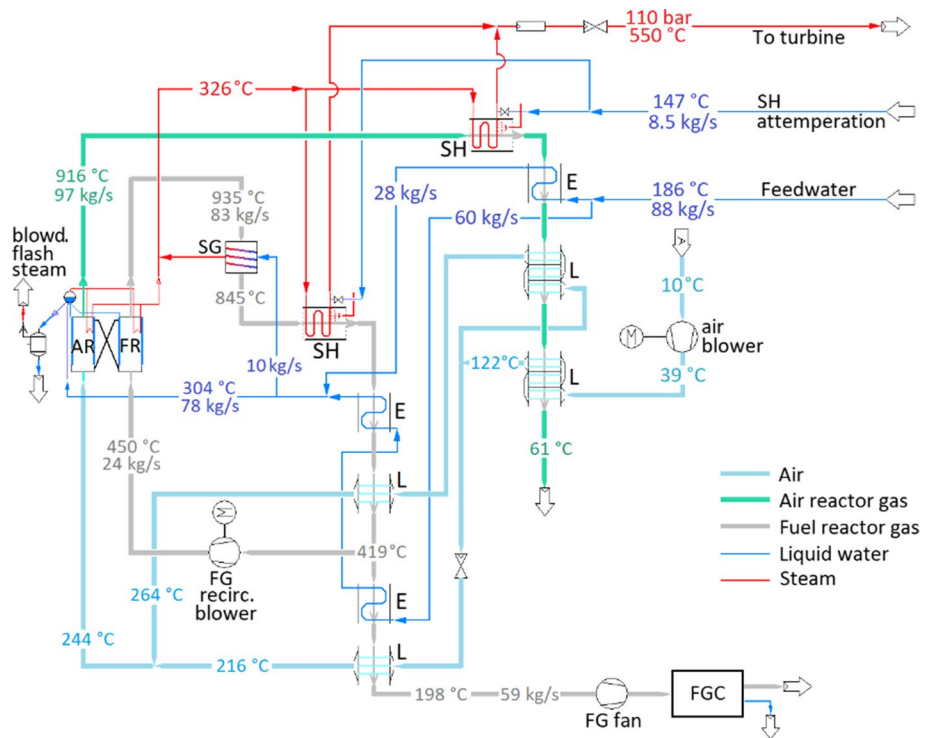


**Fig. 5** Heat transfer surface arrangement of the CLOU reactor back passes. The steam generator surfaces used for reactor wall cooling are not shown, and consecutive superheaters are depicted as single heat exchangers. AR, air reactor; FR, fuel reactor; SG, steam generator; SH, superheater; E, economizer; L, air preheater (luvo); FGC, flue gas condenser

### 3.2 Overall system performance

The main operating characteristics of the reference plant and the CLOU-CHP plant are listed in Table 7. At nominal load, the reference plant with conventional CFB boiler and 142 °C flue gas stack temperature has a thermal output of 248 MW and an electrical efficiency of  $\eta_{el}=23.8\%$ . With the same fuel input, the CLOU system yields a 321 MW thermal output (including flue gas condenser) and a practically unchanged  $\eta_{el}$  at 23.8%. The unchanged net power generation is a result of an 18 MW generator power increase and a similar increase of auxiliary power consumption almost exactly compensating for each other, yielding in fact not an efficiency penalty, but a very small 0.2 MW net power generation gain as the net outcome.

Of the auxiliary power consumption increase, approximately 2/3 is due to the CO<sub>2</sub>-CPU; considerably increased fan power consumptions are responsible for most of the rest. The flue gas condensation system auxiliary consumption is somewhat less at 1.6 MW, of which the NH<sub>3</sub> compression heat pump is responsible for approximately 90%.

### 3.3 Heat recovery and utilization

While the CLOU plant efficiency remains almost unchanged from the reference plant, the thermal power increase is considerable at 73 MW, mostly due to the condensation of water from the fuel



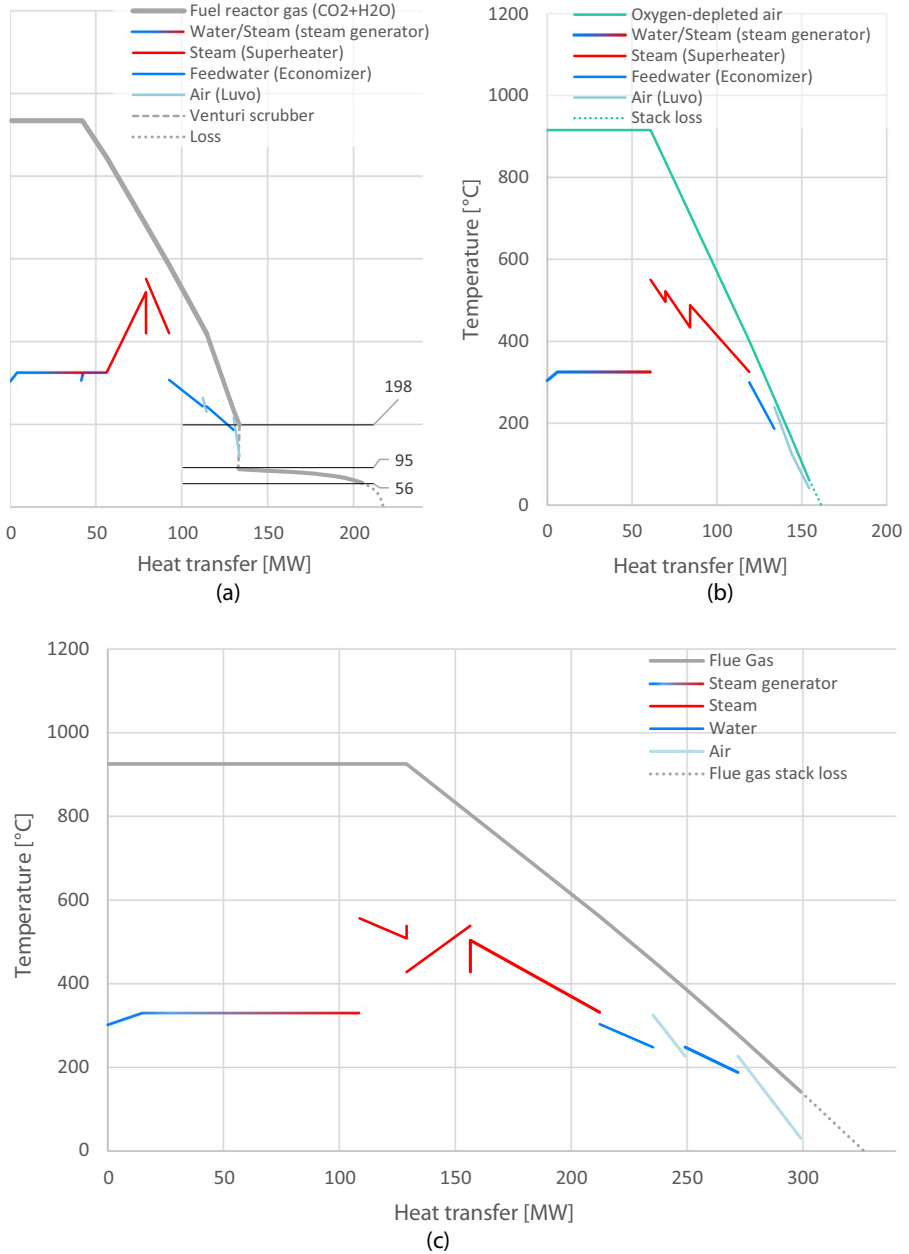


**Fig. 6** Temperature diagrams of the CLOU reactor FR (a), AR (b) and baseline power boiler replaced by the CLOU reactor system (c)

reactor gas, as well as to a lesser extent the low stack temperature of the air reactor gas flow. The benefit of condensing flue gas heat recovery would be much less in conventional boilers; the low concentration of water in typical biomass boiler flue gas limits the temperature levels to little over

**Table 6** Total conductances G (kW/K) of the different types of heat transfer surfaces in the CLOU reactor system and the reference CFB plant

Heat transfer surface	CLOU AR	CLOU FR	CFB
Steam generator, membrane wall	103	68	182
Steam generator, boiler bank	0	27	0
Superheater	330	166	334
Economizer	170	236	300
Air preheater	723	112	446

**Table 7** Performance of the BECCS power plant

Category	Parameter	Reference	CLOU
Overall performance	Fuel input ( $MW_{LHV}$ )	275.8	275.8
	Boiler thermal output ( $MW_{th}$ )	248.3	321.1
	Boiler efficiency (%)	90.0	116.4
	Net electric efficiency (%)	23.8	23.8
	Generator (MW)	70.4	88.6
	Net power (mill total) (MW)	33.1	33.3
	Stack temperature ( $^{\circ}C$ )	142	60.5/55.3 <sup>a</sup>
Ambient conditions	Air temperature <sup>b</sup> ( $^{\circ}C$ )	27	10
	Makeup water ( $^{\circ}C$ )	10	10
	Condenser cooling water ( $^{\circ}C$ )	5	5
Turbine	HPT inlet flow (kg/s)	91.6	95.6
	Condensing turbine flow (kg/s)	18.1	44.8
	Condenser pressure (mbar)	25	25
Auxiliary power consumption	Fans and blowers (MW)	1.01	5.33
	Steam cycle pumps (MW)	1.67	1.65
	Condenser cooling water pump (MW)	0.14	0.30
	Flue gas condenser (MW)	-	1.56
	CO <sub>2</sub> -CPU (MW)	-	12.04
	Other (MW)	1.90	1.90
	Total (MW)	4.72	22.76
Direct CO <sub>2</sub> emissions	Absolute (kg/s)	32.7	0.9
	Specific <sup>c</sup> (kg/MWh <sub>el,net</sub> )	1791	51
	Specific (kg/ADt <sub>pulp</sub> )	617	17
	Negative (t/h)	0	106

<sup>a</sup>AR gas stack temperature/FR gas to CO<sub>2</sub>-CPU

<sup>b</sup>Temperature of air entering the air heaters, after the forced draft fan/blower

<sup>c</sup>Emissions relative to net power from TG2 after deducting from the generator power the boiler/reactor and steam cycle auxiliaries, but not the pulp and paper mill consumption

60 °C at best. Low temperature limits the available heat sinks, and thereby the recoverable heat, or requires a high temperature lift and thereby low COP figures in heat pumps. Consequently, such equipment is not used in Finnish pulp mill power boilers, and remains rare in district heating CHP plants. In the CLOU FR gas stream, however, a water vapour partial pressure of 0.7 bar allows

heat recovery at over 80 °C temperature, considerably increasing the heat recovery potential, and reducing the need for heat pumps.

The condensing heat recovery scheme is depicted in Fig. 7. Much of the heat recovered in the flue gas condenser (FGC) was used for preheating the main condensate and demineralized makeup water streams, as well as replacing LP steam from pulp mill warm and hot water production. The net effect of these was a considerable increase in the steam available for full expansion in the condensing turbine, from 18 to almost 45 kg/s. It is thus clear that much of the generator power gain obtained depends on having a clearly larger condensing turbine and condenser.

## 4 Discussion

### 4.1 Performance results

The presented CLOU scheme proved to yield an extremely efficient CO<sub>2</sub> capture system, with no efficiency penalty compared to the conventional boiler system. The possibility to remove the already small efficiency penalty indicated in the biomass-fired CLOU CCS implementation presented in Saari et al. (2021) is due to the abundant low-temperature heat sinks where the heat recovered in the flue gas condensation can be used for replacing LP steam. This is partly due to the relatively much larger condensate stream of a pulp and paper mill cogeneration plant, where the biomass boiler is only one of two boilers sharing the same condensate system, and partly due to the mill heat users providing another heat sink. Furthermore, in this application, the replacement of LP steam allowed full expansion of saved steam from the 5 bar back pressure to the 25 mbar vacuum pressure of the condensing turbine. This provides considerably greater additional power generation than in district heat generation, where replacing steam from turbine by flue gas condenser heat recovery only permits expansion from less than 1 bar pressure on average, for a clearly lesser gain.

The remarkably good performance was achieved while conservatively assuming that the heat recovered in the FGC could only be used to replace hot water production and

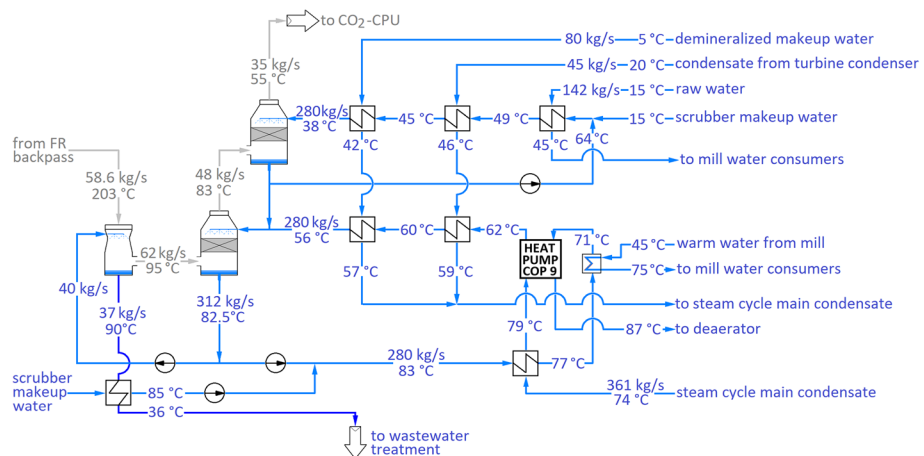


Fig. 7 Condensing heat recovery scheme

main condensate and demineralized makeup water heating in the pulp and paper mill. It is likely that in many pulp mills, some steam consumers could replace LP steam with hot water (Keshtkar et al. 2016), particularly if a heat pump was used to upgrade the heat to a higher temperature level. As the water from the lower packed bed scrubber is obtained at a fairly high temperature of 82 °C, low temperature lifts and thus high COP figures could be obtained. The high temperature level of recovered heat also opens the possibility of producing approximately atmospheric-pressure steam with a compression heat pump operating at reasonably high COP figures, further increasing the potential mill uses of the heat.

## 4.2 Carbon capture potential

Pulp and paper industry (PPI) has been identified as a large source of especially biogenic CO<sub>2</sub>, but CCS projects have so far largely focused on energy production and pulp mills have been somewhat overlooked regarding carbon infrastructure (Leeson et al. 2017). CCS has, however, been named as one of the means of PPI emission reduction by e.g. IEA (2020). Pulp mills are attractive candidates for BECCS implementation as in addition to being large point sources of biogenic CO<sub>2</sub>, they enable efficient heat integration due to existing operations and infrastructure and offer the possibility of applying BECCS without additional biomass harvesting.

The carbon capture potential of the investigated power boiler CLOU replacement is difficult to estimate precisely, as there is no source the authors are aware of that list data on pulp and paper mill power boilers. Mills can vary considerably between one another, piecemeal upgrading and expanding of existing sites, and possible combination with other types of forest industry may often result in multiple boilers located on the same site. It is also fairly common in Nordic pulp and integrated pulp and paper mills to produce energy for sale, especially to district heating of nearby communities. In such cases, the biomass-fired plant burning wood handling residues is often operated by an energy company, and is considered part of energy industry rather than pulp and paper in statistics. These boilers can be quite large in comparison to the mill and the recovery boiler, augmenting the wood handling residues used in this study with additional purchased fuels. On the other hand, especially stand-alone pulp mills without nearby energy customers may have a much smaller or even no power boiler, selling the bark instead.

While a precise evaluation of the technical carbon capture potential is not possible for the reasons described above, an estimation can nonetheless be arrived at by looking at the residues produced by wood handling, as was done in the case study here. In 2020, Nordic mills produced approximately 60%, or 16 million ADt, of the 27 M ADt of the total EU chemical pulp production. If the amount of residues per tonne of pulp was broadly similar throughout the area, this would translate to a theoretical annual biogenic carbon capture potential of 8.6 Mt of direct CO<sub>2</sub> emissions in Finland and Sweden, or 15 Mt in EU. The IEA Sustainable Development Scenario (IEA 2020) estimates CO<sub>2</sub> capture from the PPI at only 8 Mt globally in 2050, while the CO<sub>2</sub> capture from the biomass boilers of the power generation sector would be 377 Mt in 2050.

In terms of boiler capacity, the above estimate for maximum theoretical potential for carbon capture conversion in Finland would translate to 1.3 GW total capacity at 13 chemical pulp mill sites, while according to the data used in Lipiäinen et al. (2022), the actual figure is approximately 1.1 GW capacity in 6 boilers operated by the PPI. This excludes the boilers operated by energy companies at the mill sites, however, which amount to further 7 units and 1.5 GW, for a total of approximately twice the capacity in the estimate based on wood handling residues alone. Swedish situation is likely to be similar to Finland, while

boilers at mills in central and southern Europe are likely closer to the residue-based estimate, as the community heating demands are lower.

### 4.3 Captured CO<sub>2</sub>

The EU is aiming at carbon neutrality by 2050 and the European Green Deal action plan names carbon capture with storage or utilization as one of the industrial priority areas (European Commission 2019; European Parliament 2020). The main policy instrument, the EU emission trading scheme, does not yet contemplate biogenic CO<sub>2</sub> (Moya and Pavel 2018). Consequently, the cost-effectiveness of BECCS/U under the current policy must rest on the avoidance of cost of fossil CO<sub>2</sub> emissions and/or utilization of the captured CO<sub>2</sub>.

In PPI, there are several possibilities for on-site use of the CO<sub>2</sub>, e.g. lignin separation, tall oil production or precipitated calcium carbonate (PCC) production for paper mill coating material (Kuparinen et al. 2019). The realistic magnitude of these would be much less than the captured carbon dioxide, limited by practically separable lignin, amount of extractives in the wood species used and PCC needs of the paper mill. All would be unlikely to be simultaneously implemented as this would transform the mill from net electricity producer to a consumer, but even then, at most up to 10% of the 106 t/h captured CO<sub>2</sub> could be utilized (Kuparinen et al. 2019).

In the future, electrofuels can also be expected to become a significant consumer of captured CO<sub>2</sub> (Lehtonen et al. 2019). While some could be converted in on-site production using the excess electricity, converting the 106 t/h rate to for example methanol would consume 721 MW electricity (Kuparinen et al. 2021), far exceeding the net production available at the mill. Storage and transportation of the captured CO<sub>2</sub> will thus be needed, whether for permanent storage, or possible synthetic electrofuel manufacture in the future.

## 5 Summary and conclusions

This study assessed the potential of CLOU with a copper-based oxygen carrier for combined heat and power generation from biomass with CO<sub>2</sub> capture in a pulp and paper industry application. The system was assessed by combining 1.5D reactor modelling with process integration in a full-scale CHP plant model. The total performance of the CLOU-integrated CHP plant was evaluated, and both power generation efficiency and carbon capture performance were quantified. The power generation was compared with that of a conventional reference biomass boiler plant without CO<sub>2</sub> capture.

The design of the CLOU reactor system employed in this work is based on the dual circulating fluidized bed concept. A systematic procedure for the dimensioning and integration of the CLOU reactors into a large-scale power plant was followed. For the conditions that were considered in the study, the hydrodynamic operating range of the CLOU-CFB reactors appeared to be feasible and compares well to that of current CFB boilers. The reactor system showed high performance under CLOU operation as the volatile matter that was generated during biomass devolatilization was almost completely converted to CO<sub>2</sub> and H<sub>2</sub>O. Only a minor fraction of the char remained unburnt and escaped to the air reactor, resulting in total CO<sub>2</sub> capture efficiency of approximately 97% and a specific negative CO<sub>2</sub> emission of 1.7 t<sub>CO<sub>2</sub></sub>/MWh<sub>el,net</sub> from the CLOU plant after

deducting from the generator power the auxiliary power consumptions of the CLOU reactor system, FGC, CPU and TG2, but not the mill power consumption. Relative to the pulp production, the negative CO<sub>2</sub> emission from the CLOU combustion of wood residues amounts to 556 kg/ADt. This is well in excess of the typically < 100 kg/ADt direct fossil CO<sub>2</sub> emissions chemical pulping in Europe (Lipiäinen et al. 2023).

In terms of energy efficiency, the results indicate a very good performance for the CLOU plant, with no efficiency penalty compared to a conventional CFB boiler design. Earlier studies have indicated small but non-negligible efficiency penalties in fossil coal fired condensing power stations and biomass-fired district heating back pressure plants with CLOU-based CCS systems. The good performance is due to the advantageous combination of the characteristics of biomass fuel, the CLOU system and the pulp mill CHP application providing large, low-temperature heat sinks for the recovered heat. Although the efficiency gain obtained in this work was arguably negligible at only 0.2 MW, there is considerable potential to increase this to a more substantial value if the LP steam use in the mill can be replaced by hot water from the condensing heat recovery. Production of approximately atmospheric-pressure steam with a heat pump could increase the potential even further, but the magnitudes of such opportunities could vary considerably between mills.

While there are possibilities of on-site utilization of the captured CO<sub>2</sub>, and these could improve the profitability of the studied scheme, the amount of captured gas far exceeds the potential on-site uses. Most of the CO<sub>2</sub> would need to be stored and transported. In the short term, possibilities for climate change mitigation using carbon capture in the PPI centre on carbon storage and much of the economic viability would have to be achieved through avoidance of fossil fuel emission costs, augmented by possible limited local use of the CO<sub>2</sub>. In the future, synthetic electrofuel production is likely to create a demand for biogenic carbon dioxide, making this a potential sellable product and an additional revenue stream for the mill.

The economic feasibility will depend on the investment and operating costs of the system; evaluation of these was ruled beyond the scope of this study at this point. The authors are currently working on techno-economic and life cycle analyses of a cogeneration BECCS implementation based on CLOU technology in both pulp and paper and district heating roles. In addition to the costs, the ultimate viability of the proposed CLOU-based pulp mill power boiler plant will also depend heavily on the political decision-making and the future status of bioenergy, biomass utilization and capture of biogenic CO<sub>2</sub>.

**Funding** Open Access funding provided by LUT University (previously Lappeenranta University of Technology (LUT)). The authors gratefully acknowledge the funding from the Academy of Finland for the project “Role of forest industry transformation in energy efficiency improvement and reducing CO<sub>2</sub> emissions”, grant number 315019.

**Data availability** Data sharing not applicable to this article as no datasets were generated or analysed during the current study.

## Declarations

**Consent to participate** The research did not involve humans or animals.

**Competing interests** The authors declare no competing interests.

**Open Access** This article is licensed under a Creative Commons Attribution 4.0 International License, which permits use, sharing, adaptation, distribution and reproduction in any medium or format, as long as you give appropriate credit to the original author(s) and the source, provide a link to the Creative Commons licence, and indicate if changes were made. The images or other third party material in this article are included in the article's Creative Commons licence, unless indicated otherwise in a credit line to the material. If material is not included in the article's Creative Commons licence and your intended use is not permitted by statutory regulation or exceeds the permitted use, you will need to obtain permission directly from the copyright holder. To view a copy of this licence, visit <http://creativecommons.org/licenses/by/4.0/>.

## References

- Abad A, Adánez-Rubio I, Gayán P, García-Labiano F, de Diego LF, Adánez J (2012) Demonstration of chemical-looping with oxygen uncoupling (CLOU) process in a 1.5kWh continuously operating unit using a Cu-based oxygen-carrier. *Int J Greenh Gas Control* 6:189–200. <https://doi.org/10.1016/j.ijggc.2011.10.016>
- Abdulally I, Beal C, Andrus H, Eppele B, Lyngfelt A, White B (2014) Alstom's chemical looping technology program update. In 11th Annual conference on carbon capture utilization & sequestration, Pittsburgh, PA, USA, 29 July to 1 August, 2014. <https://netl.doe.gov/sites/default/files/2017-11/J-Chui-Alstom-Chemical-Looping-Combustion-Technology.pdf>. Accessed 9 January 2023
- Adánez J, Abad A, Mendiara T, Gayán P, De Diego LF, García-Labiano F (2018) Chemical looping combustion of solid fuels. *Prog Energy Combust Sci* 65:6–66. <https://doi.org/10.1016/j.pecs.2017.07.005>
- Adánez-Rubio I, Abad A, Gayán P, De Diego LF, García-Labiano F, Adánez J (2014) Biomass combustion with CO<sub>2</sub> capture by chemical looping with oxygen uncoupling (CLOU). *Fuel Process Technol* 124:104–114. <https://doi.org/10.1016/j.fuproc.2014.02.019>
- Aspelund A, Kristin J (2007) Gas conditioning – the interface between CO<sub>2</sub> capture and transport. *Int J Greenh Gas Control* 1:343–354. [https://doi.org/10.1016/S1750-5836\(07\)00040-0](https://doi.org/10.1016/S1750-5836(07)00040-0)
- Bandilla KW (2020) Carbon capture and storage. In: Letcher TM (ed) *Future energy*, 3rd edn. Elsevier, Amsterdam, Netherlands, pp 669–692
- Basu P (2006) *Combustion and gasification in fluidized bed*, 1st edn. CRC Press, Taylor & Francis Group, Boca Raton, FL, USA. <https://doi.org/10.1201/9781420005158>
- Champion WM, Cooper CD, Mackie KR, Cairney P (2014) Development of a chemical kinetic model for a biosolids fluidized-bed gasifier and the effects of operating parameters on syngas quality. *J Air Waste Manag Assoc* 64(2):160–174. <https://doi.org/10.1080/10962247.2013.845619>
- Clayton CK, Sohn HY, Whitty KJ (2014) Oxidation kinetics of Cu<sub>2</sub>O in oxygen carriers for chemical looping with oxygen uncoupling. *Ind Eng Chem Res* 53:2976–2986. <https://doi.org/10.1021/ie402495a>
- Clayton CK, Whitty KJ (2014) Measurement and modeling of decomposition kinetics for copper oxide-based chemical looping with oxygen uncoupling. *Appl Energy* 116:416–423. <https://doi.org/10.1016/j.apenergy.2013.10.032>
- Dargam FC, Perz E (1998) A decision support system for power plant design. *Eur J Oper Res* 109:310–320. [https://doi.org/10.1016/S0377-2217\(98\)00059-9](https://doi.org/10.1016/S0377-2217(98)00059-9)
- de Coninck H, Revi A, Babiker M, Bertoldi P, Buckeridge M, Cartwright A, Dong W, Ford J, Fuss S, Hourcade J-C, Ley D, Mechler R, Newman P, Revokatova A, Schultz S, Steg L, Sugiyama T (2018) Strengthening and Implementing the Global Response. In: Masson-Delmotte V, Zhai P, Pörtner H-O, Roberts D, Skea J, Shukla PR, Pirani A, Moufouma-Okia W, Péan C, Pidcock R, Connors S, Matthews JBR, Chen Y, Zhou X, Gomis MI, Lonnoy E, Maycock T, Tignor M, Waterfield T (eds) *Global Warming of 1.5°C. An IPCC Special Report on the impacts of global warming of 1.5°C above pre-industrial levels and related global greenhouse gas emission pathways, in the context of strengthening the global response to the threat of climate change, sustainable development, and efforts to eradicate poverty*. Cambridge University Press, Cambridge, UK and New York, NY, USA, pp 313–444. <https://doi.org/10.1017/9781009157940.006>
- Environmental Protection Agency (EPA) (2009) *Emerging technologies for reducing greenhouse gas emissions from the pulp and paper manufacturing industry*. US Environmental Protection Agency, Washington, DC, USA
- Ericsson K, Nilsson LJ (2018) *Climate innovations in the paper industry: prospects for decarbonisation*. In: IMES/EESS report series, vol 110. Department of Technology and Society, LTH, Lund University, Lund, Sweden
- European Commission (2019) *Communication from the Commission – The European Green Deal (COM(2019) 640 final, 11.12.2019)*. European Commission, Brussels, Belgium. <https://eur-lex.europa.eu/legal-content/EN/TXT/?uri=CELEX:52019DC0640>. Accessed 24 Sep 2022


- European Parliament (2020) European Parliament resolution of 15 January 2020 on the European Green Deal (2019/2956(RSP)). Parliament Resolution 15 January 2020, [https://www.europarl.europa.eu/doceo/document/TA-9-2020-0005\\_EN.html](https://www.europarl.europa.eu/doceo/document/TA-9-2020-0005_EN.html). Accessed 25 September 2022
- Fajardy M, Morris J, Gurgel A, Herzog H, Mac Dowell N, Paltsev S (2021) The economics of bioenergy with carbon capture and storage (BECCS) deployment in a 1.5 C or 2 C world. *Glob Environ Change* 68:102262. <https://doi.org/10.1016/j.gloenvcha.2021.102262>
- Hamaguchi M, Saari J, Vakkilainen E (2013) Bio-oil and biochar as additional revenue streams in South American kraft pulp mills. *BioResources* 8(3):3399–413. <https://doi.org/10.15376/biores.8.3.3399-3413>
- Häggestahl D, Dahlquist E (2003) Evaluation of Prosim and IPSEpro, two heat and mass balance simulation softwares. In: Proceedings of the SIMS conference on simulation and modelling. SIMS, Västerås, Sweden, pp 221–226
- Ikonen O (2013) Improving energy efficiency of biomass power plant and optimizing partial-load operation (in Finnish: Biovoimalaitoksen energiätehokkuuden parantaminen ja osakuorma-ajon optimointi). M.Sc. Thesis, Lappeenranta University of Technology, Lappeenranta, Finland
- International Energy Agency (IEA) (2020) Special report on carbon capture, utilisation and storage: CCUS in clean energy transitions. International Energy Agency, Paris
- International Energy Agency (IEA) (2022) Pulp and paper, international energy agency. <https://www.iea.org/fuels-and-technologies/pulp-paper>. Accessed 22 Sep 2022
- Jüdes M, Vigerske S, Tsatsaronis G (2009) Optimization of the design and partial-load operation of power plants using mixed-integer nonlinear programming. In: Kallrath J, Pardalos PM, Rebennack S, Scheidt M (eds) Optimization in the energy industry, energy systems. Springer, Berlin Heidelberg, Berlin, Heidelberg, pp 193–220. [https://doi.org/10.1007/978-3-540-88965-6\\_9](https://doi.org/10.1007/978-3-540-88965-6_9)
- Karjunen H, Tynjälä T, Hyppänen T (2017) A method for assessing infrastructure for CO<sub>2</sub> utilization: a case study of Finland. *Appl Energy* 205:33–43. <https://doi.org/10.1016/j.apenergy.2017.07.111>
- Kearns D, Liu H, Consoli C (2021) Technology readiness and costs of CCS, <https://www.globalccsinstitute.com/resources/publications-reports-research/technology-readiness-and-costs-of-ccs/>. Accessed 22 September 2022
- Keshtkar M, Ammara R, Perrier M, Paris J (2016) Thermal energy efficiency analysis and enhancement of three Canadian Kraft mills. *J Sci Technol Forest Products Process* 5:24–60
- Kuparinen K, Vakkilainen E, Tynjälä T (2019) Biomass-based carbon capture and utilization in kraft pulp mills. *Mitig Adapt Strateg Glob Chang* 24:1213–1230. <https://doi.org/10.1007/s11027-018-9833-9>
- Kuparinen K, Lipiäinen S, Vakkilainen E (2021) Can carbon capture be a new revenue opportunity for the pulp and paper sector? *Tappi J* 20(8):527–540
- Leeson D, Mac Dowell N, Shah N, Petit C, Fennell P (2017) A Techno-economic analysis and systematic review of carbon capture and storage (CCS) applied to the iron and steel, cement, oil refining and pulp and paper industries, as well as other high purity sources. *Int J Greenh Gas Control* 61:71–84. <https://doi.org/10.1016/j.ijggc.2017.03.020>
- Lehtonen J, Järnefelt V, Alakurtti S, Arasto A, Hannula I, Harlin A, Koljonen T, Lantto R, Lienemann M, Onarheim K, Pitkänen JP (2019) The carbon reuse economy: transforming CO<sub>2</sub> from a pollutant into a resource. VTT Technical Research Centre of Finland. <https://doi.org/10.32040/2019.978-951-38-8709-4>
- Lipiäinen S, Apajalahti E-L, Vakkilainen E (2023) Decarbonization prospects for the european pulp and paper industry: different development pathways and needed actions. *Energies* 16:746. <https://doi.org/10.3390/en16020746>
- Lipiäinen S, Kuparinen K, Sermiyagina E, Vakkilainen E (2022) Pulp and paper industry in energy transition: towards energy-efficient and low carbon operation in Finland and Sweden. *Sustain Prod Consum* 29:421–431. <https://doi.org/10.1016/j.spc.2021.10.029>
- Mattisson T (2013) Materials for chemical-looping with oxygen uncoupling. *ISRN Chem Eng* 2013:526375. <https://doi.org/10.1155/2013/526375>
- Mattisson T, Lyngfelt A, Leion H (2009) Chemical-looping with oxygen uncoupling for combustion of solid fuels. *Int J Greenh Gas Control* 3:11–19. <https://doi.org/10.1016/j.ijggc.2008.06.002>
- Moya JA, Pavel CC (2018) Energy efficiency and GHG emissions: prospective scenarios for the pulp and paper industry. Publications Office of the European Union, Luxembourg. <https://doi.org/10.2760/035301>
- Onarheim K, Santos S, Kangas P, Hankalin V (2017a) Performance and costs of CCS in the pulp and paper industry Part 1: Performance of amine-based post-combustion CO<sub>2</sub> capture. *Int J Greenh Gas Control* 59:58–73. <https://doi.org/10.1016/j.ijggc.2017.02.008>
- Onarheim K, Santos S, Kangas P, Hankalin V (2017b) Performance and cost of CCS in the pulp and paper industry Part 2: Economic feasibility of amine-based post-combustion CO<sub>2</sub> capture. *Int J Greenh Gas Control* 66:60–75. <https://doi.org/10.1016/j.ijggc.2017.09.010>
- Peltola P, Ritvanen J, Tynjälä T, Pröhl T, Hyppänen T (2013a) One-dimensional modelling of chemical looping combustion in dual fluidized bed reactor system. *Int J Greenh Gas Control* 16:72–82. <https://doi.org/10.1016/j.ijggc.2013.03.008>



- Peltola P, Ritvanen J, Tynjälä T, Hyppänen T (2013b) Model-based evaluation of a chemical looping combustion plant for energy generation at a pre-commercial scale of 100 MW<sub>th</sub>. *Energy Convers Manag* 76:323–331. <https://doi.org/10.1016/j.enconman.2013.07.062>
- Peltola P, Ritvanen J, Tynjälä T, Hyppänen T (2015) Fuel reactor modelling in chemical looping with oxygen uncoupling process. *Fuel* 147:184–194. <https://doi.org/10.1016/j.fuel.2015.01.073>
- Peltola P, Saari J, Tynjälä T, Hyppänen T (2020) Process integration of chemical looping combustion with oxygen uncoupling in a biomass-fired combined heat and power plant. *Energy* 210:118550. <https://doi.org/10.1016/j.energy.2020.118550>
- Peltola P, Alobaid F, Tynjälä T, Ritvanen J (2022) Overview of fluidized bed reactor modeling for chemical looping combustion: status and research needs. *Energy Fuels* 36:9385–9409. <https://doi.org/10.1021/acs.energyfuels.2c01680>
- Saari J, Kuparinen K, Sermyagina E, Vakkilainen E, Kaikko J, Sergeev V (2018) Effect of integration method and carbonization temperature on the performance of an integrated hydrothermal carbonization and CHP plant. *BioResources* 13:5080–5110
- Saari J, Sermyagina E, Kaikko J, Haider M, Hamaguchi M, Vakkilainen E (2021) Evaluation of the energy efficiency improvement potential through back-end heat recovery in the kraft recovery boiler. *Energies* 14:1550. <https://doi.org/10.3390/en14061550>
- Saari J, Peltola P, Tynjälä T, Hyppänen T, Kaikko J, Vakkilainen E (2020) High-efficiency bioenergy carbon capture integrating chemical looping combustion with oxygen uncoupling and a large cogeneration plant. *Energies* 13:3075. <https://doi.org/10.3390/en13123075>
- Sanders WP (2004) Turbine steam path Vol. IIIa: mechanical design and manufacture. PennWell Books, Tulsa, OK, USA
- Schlosser F, Jesper M, Vogelsang J, Walmsley TG, Arpagaus C, Hesselbach J (2020) Large-scale heat pumps: applications, performance, economic feasibility and industrial integration. *Renew Sustain Energy Rev* 133:110219. <https://doi.org/10.1016/j.rser.2020.110219>
- Spinelli M, Peltola P, Bischì A, Ritvanen J, Hyppänen T, Romano MC (2016) Process integration of chemical looping combustion with oxygen uncoupling in a coal-fired power plant. *Energy* 103:646–659. <https://doi.org/10.1016/j.energy.2016.02.167>
- Ströhle J, Orth M, Epple B (2014) Design and operation of a 1 MW<sub>th</sub> chemical looping plant. *Appl Energy* 113:1490–1495. <https://doi.org/10.1016/j.apenergy.2013.09.008>
- Toftegaard MB, Brix J, Jensen PA, Glarborg P, Jensen AD (2010) Oxy-fuel combustion of solid fuels. *Prog Energy Comb Sci* 36(5):581–625. <https://doi.org/10.1016/j.peccs.2010.02.001>
- Traupel W (1966) Thermal Turbomachinery: 1. Thermodynamic - fluid mechanics calculation (In German: Thermische Turbomaschinen: 1. Thermodynamisch-Strömungstechnische Berechnung). Springer, Berlin/Heidelberg, Germany.
- Vakkilainen E (2005) Kraft recovery boilers—principles and practice, 2nd edn. Finnish Recovery Boiler Association/Suomen Soodakattilayhdistys r.y., Helsinki, Finland
- Vakkilainen E, Kuparinen K, Heinimö J (2013) Large industrial users of energy biomass. IEA Bioenergy Task 40. <https://www.ieabioenergy.com/publications/large-industrial-users-of-energy-biomass/>. Accessed 22 Sep 2022
- Vakkilainen E, Kivistö A (2014) Forest industry energy consumption – trends and effects of modern mills. Lappeenranta University of Technology, Lappeenranta
- Whitty K (2012) Practical challenges of system design for a CLOU-based system for chemical looping combustion of coal. In: Proceedings of the 2nd International Conference on Chemical Looping. ICCL, Darmstadt, Germany

**Publisher's note** Springer Nature remains neutral with regard to jurisdictional claims in published maps and institutional affiliations.

## Authors and Affiliations

Jussi Saari<sup>1</sup>  · Petteri Peltola<sup>1</sup> · Katja Kuparinen<sup>1</sup> · Juha Kaikko<sup>1</sup> · Ekaterina Sermyagina<sup>1</sup> · Esa Vakkilainen<sup>1</sup>

Petteri Peltola  
petteri.peltola@endev.fi

Katja Kuparinen  
katja.kuparinen@lut.fi

Juha Kaikko  
juha.kaikko@lut.fi

Ekaterina Sermyagina  
sermyagina.ekaterina@gmail.com

Esa Vakkilainen  
esa.vakkilainen@lut.fi

<sup>1</sup> School of Energy Systems, Lappeenranta-Lahti University of Technology LUT, P.O. Box 20, 53851 Lappeenranta, Finland